CTU Journal of Innovation and Sustainable Development
ISSN 2615-9422 | e-ISSN 2815-5602

DOI:10.22144/ctujoisd.2024.261

NaY zeolite synthesis from rice husk ash for Chromium(VI) ion adsorption

Luong Huynh Vu Thanh[1,2*], Nguyen Hoang Ngoan[1,3], Pham Thi Kim Thu[1,3], Le Thanh Phu[1,4], Le Tran Lan Trinh[1,4], Dang Huynh Giao[1,2], and Tran Thi Bich Quyen[2]

[1]*Applied Chemical Engineering Lab, College of Engineering, Can Tho University, Viet Nam*

[2]*Faculty of Chemical Engineering, College of Engineering, Can Tho University, Viet Nam*

[3]*Course-46 student, Faculty of Chemical Engineering, College of Engineering, Can Tho University, Viet Nam*

[4]*Course-45 student, Faculty of Chemical Engineering, College of Engineering, Can Tho University, Viet Nam*

**Corresponding author (lhvthanh@ctu.edu.vn)*

Article info.

Received 06 Sep 2023
Revised 19 Sep 2023
Accepted 26 Sep 2023

Keywords

Adsorbent, adsorption, chromium (VI), NaY zeolite, rice husk ash

ABSTRACT

NaY zeolite in this study is novelly synthesized from rice husk ash with a one-stage process instead of passing the solid silica recovery process as usual. NaY zeolite applies to assess adsorption ability of chromium(VI) ions in water with varying key factors. The as-synthesized zeolite is characterized by X-ray diffraction, X-ray fluorescence, scanning electron microscope, specific surface area analysis and inductively coupled plasma mass spectrometry with optical emission spectroscopy. As a result, the optimal conditions for silica extraction are at 90°C with a NaOH concentration of 4 M for 4 h with recovery efficiency 87.5%. NaY zeolite is successfully synthesized with Si/Al ratio of 10, aging time of 24 h and crystallization time of 24 h with synthesis yield of 31.25% and crystallinity of 96%. The optimal conditions for the chromium(VI) adsorption in aqueous solution are at pH 2.0, adsorption time of 120 min, initial concentration of 20 mg/L with an adsorbent mass of 0.1 g. The kinetics and adsorption isotherms show a good agreement with pseudo-second order and Freundlich adsorption isotherm model. NaY zeolite is synthesized via environmentally friendly approach with time and energy savings and shows its high adsorb-ability of chromium(VI) in water.

1. INTRODUCTION

Increasing population and industrialization is occurring fast and causing water pollution in developing countries. One of the major challenges in water or wastewater treatment is heavy metal contamination (Sharma et al., 2022). Metals, namely mercury (Hg), chromium (Cr), lead (Pb), arsenic (As), cadmium (Cd), nickel (Ni), etc., are listed as heavy metals since their density is higher than 5 $g.ml^{-1}$ (Shrestha et al., 2021). One of them, hexavalent chromium (Cr(VI)), is a highly toxic metal ion used in various industries such as tanning, stainless steel manufacture, electroplating, and so on (Dzyazko et al., 2007). When Cr(VI) ion is released into the environment, it has a significant influence on the health of creatures and people like lung cancer, skin, liver, and kidney damage, or gastrointestinal problems (Sharma et al., 2022). As a result, it is critical to discover an efficient method to remove Cr(VI) ion in effluents.

Many methods have been used to remove Cr(VI) ion from aqueous solution, including adsorption, ion-exchange, chemical reduction and membrane filtration, and adsorption is one of the most popular

techniques attracting many researchers because it is simple, low-cost, reliable and highly efficient (Mahmoud et al., 2021). In the adsorption method, the adsorbent plays an essential role in removing contaminants. Adsorbents such as clays, activated carbon, bio-mass derivatives like coconut shell charcoal, paper wastes, biochar-based composites, have been researched to absorb Cr(VI) ion from aqueous solution (Alemu et al., 2018; Alemu et al., 2020; Imran, 2020). These adsorbents are normally low thermal stability, selectivity and adsorption ability (Murtaza et al., 2023). Therefore, zeolite stands out as a potential candidate for removal heavy metals because of its high surface area, porosity percentage and cation exchange capacity (Álvarez et al., 2021).

Zeolites are water containing crystalline alumino-silicates made of TO_4 tetrahedral (T = Al, Si), with each atomic oxygen peak sharing a tetrahedron (Auerbach et al., 2003). As a member of zeolite family, synthetic zeolite Y is a very adaptable Faujasite zeolite molecular sieve with a 7.4 structure, three dimensions, and solid acidity that makes it effective as a catalyst, ion exchanger, and adsorbent (Zeevi et al., 2012). Zeolite Y can be synthesized from different silicon sources such as kaolin, clay, coal fly ash, rice husk ash and other sources (Derbe et al., 2021; Saceda, 2011). Among these sources, rice husk ash (RHA) has attracted the interests of researchers for using it as a silicon source for zeolite synthesis (Ali et al., 2011; Flores, 2021; Kordatos et al., 2008; Wang, 2019). RHA has a content of SiO_2 in both amorphous and crystalline depending on the combustion techniques (Hamad & Khattab, 1981). To increase the content of SiO_2 in RHA, hence, it has to be burned at high temperature (≥750°C) for some hours (≥6h) (Tan et al., 2011). This step is attributed to increase energy consumption during synthesizing zeolite from RHA. Therefore, it is critical to address the reduction of energy consumption for zeolite synthesis.

The main objective of this work is to synthesize zeolite using RHA as a silicone source after extracting it as a sodium silicate solution without using heat pretreatment or recovering it into solid silica form. This study also examines how sodium hydroxide content, temperature, and time affect silica recovery from rice husk ash, as well as how crystallization time and aging time influence the zeolite synthesis. Furthermore, the adsorption capacity of chromium(VI) ion from aqueous solution using as-synthesized NaY zeolite is conducted under the effect of pH, contact time, and initial concentration. Besides, the kinetics and adsorption isotherms are applied to evaluate the adsorption of Cr(VI) on the NaY zeolite.

2. MATERIALS AND METHOD

2.1. Chemicals and materials

Rice hush ask is obtained from Duc An brick kiln, My Xuong ward, Cao Lanh district, Dong Thap province. Chlohydric acid (HCl 36-38%), Sodium hydroxide (NaOH 96%), Potassium dichromate ($K_2Cr_2O_7$ >97%) are provided by Xilong Chemicals, China. Sodium aluminate ($NaAlO_2$ >99%) is obtained from Tianqin Chemicals, China. Distilled water is from Applied Chemical Engineering lab, Can Tho University.

2.2. Zeolite NaY synthesis

The synthesis of NaY zeolite from RHA consists of three main steps, namely pretreatment, silica recovery and zeolite synthesis. To this end, the RHA is first cleaned and dried before soaking in 2 M HCl solution for 24 h. After soaking, RHA is filtered, neutralized, and dried at 100°C for 6 h, but skipping the calcination step to save time and energy. This method aims to remove metal ions from RHA before synthesizing zeolite (Wittayakun et al., 2008).

After pretreatment, the 10 g of RHA is respectively refluxed with 50 mL NaOH at concentrations of 3 M, 4 M and 5 M, temperatures of 70°C, 80°C, 90°C and 100°C, and time intervals of 3 h, 4 h and 6 h. The experiment is carried out using the approach of alternating each variable to determine the best values for the influencing factors. This step is to determine the optimum conditions for silica recovery. After boiling, the sodium silicate solution (solution 1) will be filtered and applied to synthesize zeolite NaY. This one-pot method aims to avoid adding acid to recover solid SiO_2 causing time and chemical consumption (Saceda et al., 2011).

Before synthesizing NaY zeolite, 50 mL of the sodium silicate solution (solution 1) is placed into a beaker. Sodium aluminate solution is then prepared by stirring 1.79 g $NaAlO_2$ into 20 mL of water until totally dissolved. Then, the sodium aluminate solution is gradually added to solution 1 and stirred until get a homogenous mixture (mixture 1). The mixture 1 is aged for 12 h, 24h and 48 h and crystallized in 12 h, 24 h, 48 h and 72 h at 110°C, respectively. The as-synthesized NaY zeolite is then rinsed to neutral and dried at 80°C for 24 h. Each experiment in this study is triplicated.

2.3. Zeoilte NaY characterizations

The synthetic NaY zeolite is characterized using different advanced analysis methods. In details, X-ray fluorescence spectroscopy (XRF, Horiba MESA-50) is used to evaluate the chemical composition of RHA. Inductively coupled plasma mass spectrometry with optical emission spectroscopy (ICP-OES, ICAP7400DUO-SPH006) is employed to measure the SiO_2 content of Na_2SiO_3 solution. The structures of RHA and NaY zeolite are examined using X-ray diffraction (XRD, Empyrean/ PANalytical). The NaY zeolite morphology is investigated using diffraction field emission associated scanning electron microscopy (FE-SEM) data obtained with a Hitachi S-4800 equipment. A Quantachromenha gas adsorption analyser (NOVA: 4000e) is used to evaluate the zeolite's specific surface area, pore volume, and pore size.

The surface charge of NaY zeolite is determined by using the salt method (Khan & Sarwar, 2007). Firstly, fill beaker with 20 mL of 0.1 M KCl solution and adjust the pH to 11 using 0.01 M NaOH and 0.01 M HCl. Place 0.1 g of NaY zeolite into several beakers with pH ranging from 2 to 11 on a shaker. After 24 h, take a pH reading of the solution. The difference in pH between the solution's before and after 24 h shows the surface charge of zeolite at various pH points and the point of zero charge of zeolite (pH_{pzc}).

2.4. Chromium(VI) adsorption by zeolite NaY

To examine the parameters that influence Cr(VI) adsorption, the following parameters are investigated: pH (2-6), adsorption time (0.5 to 6 h), and initial Cr(VI) concentration (10-30 mg/L). To this end, a stock of Cr(VI) solution (1000 mg/L) is prepared by dissolving $K_2Cr_3O_7$ in distilled water. All working solutions are prepared from the stock solution by diluting with distilled water. The pH adjustment is conducted by using 0.01 M HCl and 0.01 M NaOH solution.

Concentrations of Cr(VI) are measured by using a UV-Vis spectrophotometer at λ = 540 nm. Adsorption capacity q (mg/g) and adsorption efficiency (%) are calculated using formulae (1) and (2) (Ghosh et al., 2013):

$$q = \frac{(C_o - C_e).V}{m} (mg/g) \quad (1)$$

$$H = \frac{C_o - C_e}{C_o} (\%) \quad (2)$$

Where C_o is the initial concentration (mg/L), C_e is the concentration remaining after adsorption (mg/L). V is the volume of the solution (L), m is the mass of the adsorbent (g).

Adsorption kinetics is an essential metric in wastewater treatment because it predicts the rate of trash adsorption in wastewater solution. In this work, kinematics equations of first (PFO) and second order (PSO) linear form are employed. Adsorption of Cr(VI) by NaY zeolite is evaluated by using the Langmuir, Freundlich, Dubinin - Radushkevich, and Temkin adsorption isotherm models (Dada et al., 2012).

3. RESULTS AND DISCUSSION

3.1. RHA characteristics

The original physicochemical composition of RHA is presented in Table 1. A very large content of SiO_2 is 94.7%, with the residual content of various other metals oxides such as Cr_2O_3, MgO, Fe_2O_3, CaO, accounting for 5.33%. The content of SiO_2 in this study is higher than that of some previous reports showing the content of SiO_2 varies from 85%-90% depending on combustion technique (Hadipramana et al., 2016; Singh, 2018). Some metal oxides are eliminated during the pretreatment process with HCl solution, including MgO from 0.258% to 0.240%, K_2O from 2.48% to 1.69%, and CaO from 0.708% to 0.349%, resulting in an increase in SiO_2 content in RHA from 94.7% to 96.5%. The major purpose of this technique is to clean other reduced functional metals. This increases SiO_2 recovery while decreasing the influence of other metal ions on zeolite production, contributing to the creation of purer zeolite.

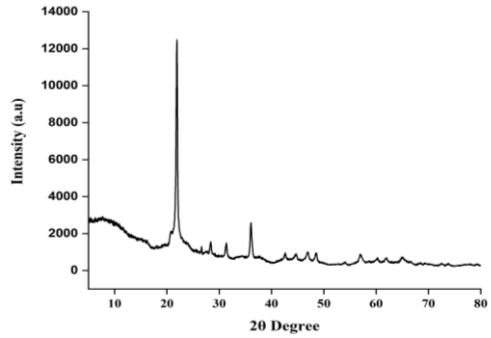

Figure 1. X-ray diffraction pattern of RHA after pretreatment

XRD analysis is used to determine the allotropic form of pre-treated RHA and the result is shown in Figure 1. The XRD result of SiO_2 from RHA in

Figure 1 demonstrates that only a broad SiO_2 peak arises at an angle of $2\theta = 22^o$ and silica can be seen in crystalline form in the pre-treated material (Singh et al., 2018). The XRF result in Table 1 confirms the high silica content of RHA, accounting for over 95% in total. This leads to the conclusion that RHA is a good material for zeolite production

Table 1. Metal oxides of RHA before and after calcination

Oxide	Initial content (%)	Final content (%)
SiO_2	94.7	96.5
K_2O	2.48	1.69
Cr_2O_3	0.017	0.059
MgO	0.285	0.240
Al_2O_3	0.504	0.296
P_2O_5	0.507	0.192
CaO	0.708	0.349
Fe_2O_3	0.224	0.250
Others	0.608	0.402

3.2. Recovery of silicate dioxide from RHA

When the temperature of NaOH solution increases, a rise of SiO_2 recovery yield is observed and presented in Figure 2. According to the findings presented in Figure 2, at 70°C, the yield is 71.3%, and rises to 76.4% as temperature increases to 80°C. The yield increases by 5.1% when increasing temperature to 90°C and keeping the yield almost constant at 82% as the temperature rises to 100°C. As observed, temperature has a positive effect on recovery efficiency. The recovery process is essentially a solid-liquid extraction process, thus as the temperature rises, the solvent's viscosity drops, allowing the solvent to more readily enter the RHA and thereby improving the extraction capacity (Mirmohamadsadeghi & Karimi, 2020). The performance does not vary significantly between 90 and 100°C; hence, the temperature of 90°C is chosen for further experiment.

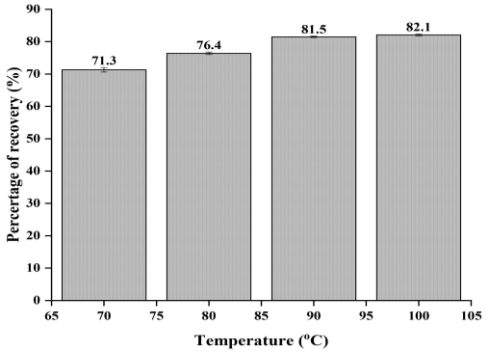

Figure 2. Effect of NaOH solution temperature (m_{RHA}=10 g, V_{NaOH}=100 mL, C_{NaOH}=4 M, t=3 h).

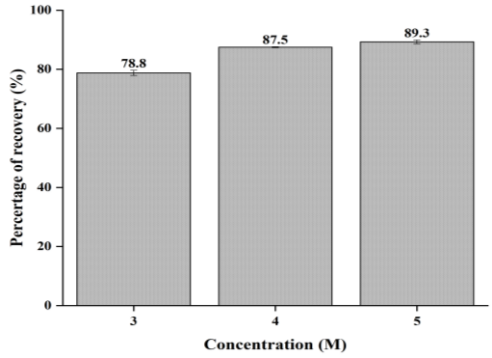

Figure 3. Effect of NaOH solution concentration (m_{RHA}=10 g, V_{NaOH}=100 mL, T=90°C, t=3 h).

Concentration of NaOH solution has a strong effect on SiO_2 recovery yield and the detailed results are presented in Figure 3. Firstly, at 3 M concentration of NaOH, the recovery yield is 78.8% when the NaOH concentration reaches 4 M, the recovery yield rises to 87.5%, and continuously to 89.3% as the concentration is at 5 M. In total, an increase of 10.45% is obtained when the concentration goes from 3 M to 5 M. When NaOH concentration is high, there are more hydroxide group in solution, attributing to the increase in SiO_2 dissolution (Haq et al., 2014). The concentration of NaOH solution in this study is higher than that of the previous report (Haq et al., 2014) since SiO_2 in this work is crystalline while SiO_2 was amorphous in the other work. However, the viscosity of the solution at high concentration of NaOH becomes significant, causing a trouble in RHA dispersion into NaOH solution. Besides that, the increase in SiO_2 recovery yield between 4 M and 5 M NaOH solution is unremarkable. Thus, 4 M NaOH is selected as an optimal concentration for further experiments. Associating with temperature and NaOH concentration, reaction time plays an important role in SiO_2 dissolution reaction. The result of reaction time affecting on SiO_2 recovery yield is depicted and shown in Figure 4. The reaction time of 3 h recovers 80.1% of SiO_2 from RHA, and when the time increases to 4 h, the recovery yield is 87.5%. If reaction time extents to 6 h, the recovery yield gets higher and reaches almost 90%. However, this extension of reaction time just makes an insignificant change in the recovery yield. Similar tendency of effect of reaction time on SiO_2 recovery yield is observed at the study of Haq et al. (2014). Thus, reaction time in this work influences the recovery process of SiO_2 from RHA and reaches an optimal value at 4 h. Finally, the optimal condition for silica recovery is at 90°C with a NaOH

concentration of 4 M over a time period of 4 h with recovery efficiency 87.5%.

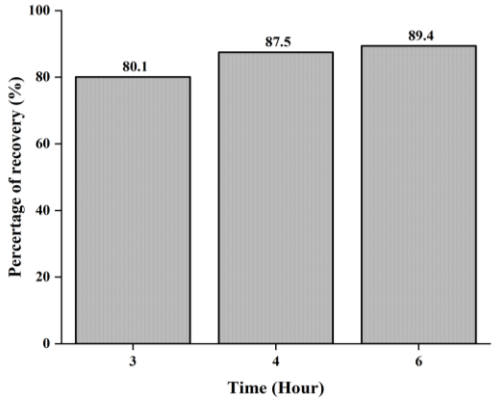

Figure 4. Effect of reaction time (m_{RHA}=10 g, V_{NaOH}=100 mL, T=90°C, C_{NaOH}=4M)

3.3. NaY zeolite synthesis

Aging time is a main element influencing the creation and development of NaY zeolite crystals. The aging intervals investigated in this study are 12 h, 24 h and 48 h, and the results are presented in Figure 5. The XRD results in Figure 6 demonstrates that at the aging time Figure 5(a) 12 h, the only peak with a low intensity appears at an angle of 2θ=27°, primarily caused by the domination of amorphous phase, showing that this aging time is insufficient for NaY zeolite crystal nucleation. The XRD findings at the aging time of 24 h (Figure 5(b)) show that some similarities to the standard NaY zeolite at 2θ values of 6.73°, 10.91°, and 23.23° (Derbe et al., 2021). These distinctive peaks of NaY zeolite appear with clearly high intensity shows because of excellent crystal nuclei formation, and the crystallinity of NaY zeolite is found to be 96%. In Figure 5(c), the peak intensity of zeolite NaY reduced after 48 h of aging, with the crystallinity of NaY zeolite obtaining only 46%. In the meantime, the distinctive peaks of NaP zeolite with high intensity appear, and its crystallinity gets to 53%. This result might be explained because a phase transition occurs throughout the aging process, causing the peak intensity of NaY to diminish and the progressive development of NaP. As a result, increasing the aging time will enhance NaP zeolite nucleation rather than NaY crystal nucleation, leading to the conclusion that the optimum aging time for NaY zeolite synthesis is 24 h.

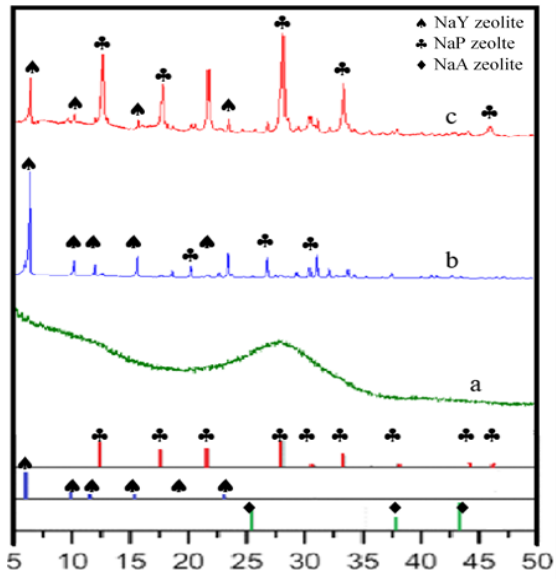

Figure 5. XRD patterns of different aging times at (a) 12 h, (b) 24 h, and (c) 48 h

Crystallization time is also an essential factor NaY zeolite crystalline development. This work examines this effect via changing crystallization time from 12 to 72 h, and presents its performance in Figure 6. As seen from Figure 6(a), because of the insufficient crystallization time of 12 h, the typical peaks of NaY zeolite appear at low intensity with the crystallinity of 37%. In addition, there are some NaP zeolite peaks found at this time, this observation is also found in the study of Mohamed et al. (2015) since this is a one-pot process (Mohamed et al., 2015). When the crystallization time is short, the NaY zeolite is not enough to form a complete structure, resulting in low crystallinity strength. The XRD results obtained after 24 h of crystallization in Figure 6(b) show that the NaY zeolite peak has high crystallinity and clarity with 96% crystallinity because of strong crystal growth. The crystallization time has a strong influence on the crystallization of NaY zeolite crystals; however, when the crystallization time is long, the crystallization intensity of NaY zeolite decreases and NaP zeolite appears. At crystallization of 48 h in Figure 6(c), the intensity of the NaY zeolite tends to lower the crystallinity of NaY to just 25%, while the NaP zeolite peaks increase with a high intensity and a crystallinity of 74%. When the crystallization time is at 72 h, the peaks of NaY zeolite had almost totally vanished, leaving only clear NaP zeolite peaks with the crystallinity up to 98%. These findings reveal the presence of only NaP zeolite without the presence of NaA zeolite. As a result, it

can be inferred that a 24-h-aging time and a 24-h-crystallization time are the optimum time for the synthesis of NaY zeolite with NaY zeolite yield of 31.25%.

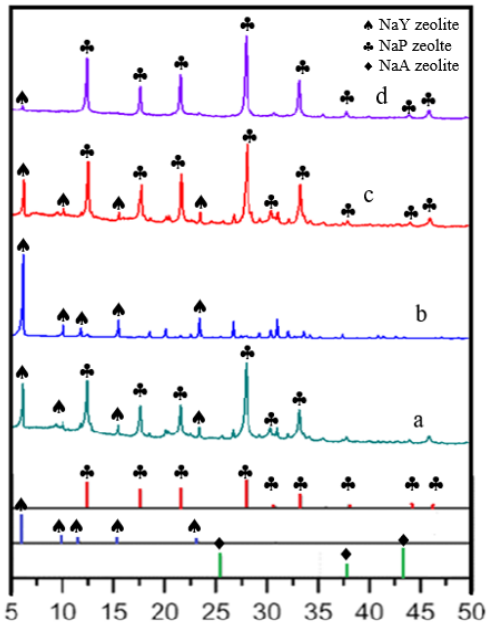

Figure 6. XRD patterns of different crystallization times at (a) 12 h, (b) 24 h, (c) 48 h, and (d) 72 h.

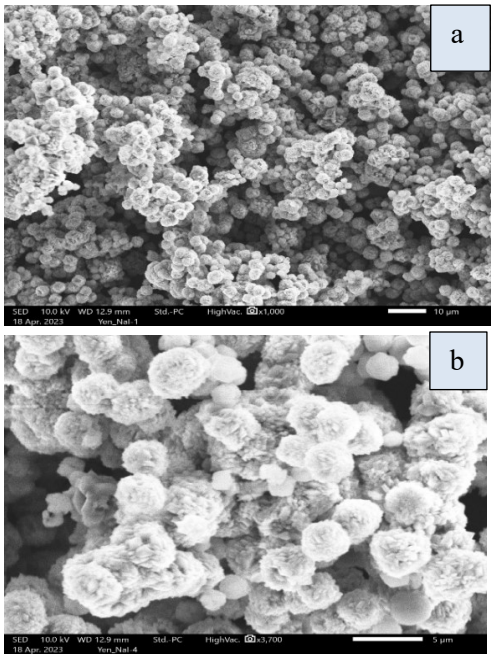

Figure 7. FE-SEM images of NaY zeolite with different resolution at (a) x1,000 and (b) x3,700

The surface morphology of NaY zeolite is assessed using field emission scanning electron microscopy, as illustrated in Figure 7. The morphology of NaY zeolite in Figure 7(a) shows that particles of NaY zeolite are uniform in size and also apparently fuse forming agglomerate particles (Figure 7(b)) (Mohamed et al., 2015). Theses agglomerate particles has average diameters in range of 3-5 micron. Due to this agglomeration of NaY zeolite particles, the BET specific surface area of NaY zeolite in this study is 164.4 m^2/g, which is lower than surface area of NaY zeolite in study of Mohamed et al., (2015), which is 406.6 m^2/g. Besides, the pore diameter and pore volume of NaY zeolite are 1.195 nm and 0.08 cm^3/g, respectively, which exhibits type-I isotherms and characteristics of microporous materials.

Besides surface morphology, surface charge of NaY zeolite is an important characteristic of adsorbent. Figure 8 shows surface charge of NaY zeolite changing from positive to negative when pH increases from 2.0 to 10.0 with the pH_{pzc} of 6.5. The result shows that the material can adsorb anions at pH less than 6.5 and adsorb cations at pH higher than 6.5.

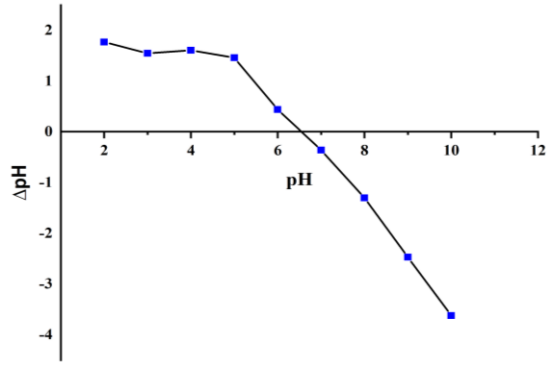

Figure 8. pH_{pzc} of NaY zeolite

3.4. Chromium(VI) ions adsorption using NaY zeolite

3.4.1. Effect of pH

In adsorption of metal ions, pH always plays a critical role; hence, the effect of pH on Cr(VI) in this study also conducts in range of 2.0 to 6.0 based on the pH_{pzc} of NaY zeolite. The effect of pH on the adsorption process is shown in Figure 9, showing that the adsorption efficiency decreases as the pH increases. At pH 2.0, the adsorption efficiency is 62.9%, and drops to 53.3% at pH 3.0. Further increases to pH 4.0, adsorption efficiency continuously decreases to 43.3%. This decrease

becomes significant when pH rises to 6.0. Similarly, the adsorption capacity drops from 2.52 mg/g at pH 2.0 to 0.71 mg/g at pH 6.0. These observations are caused by the fact that pH increase leads to decrease in positive charges on surface of the absorbent, and rise the number of hydroxide group in solution as well (Quintelas et al, 2009). Moreover, based on speciation of Cr(VI) ion, Cr(VI) ion is dominant in $Cr_2O_7^{2-}$ form, and small amount of $HCrO_4^-$ species in pH range of 1.0 – 5.6. Above pH 5.6, the amount of $Cr_2O_7^{2-}$ species decreases while that of CrO_4^{2-} increases, and both of them obtain the same quantity at pH 7.2 (Thanh et al., 2020). From the above information, one $Cr_2O_7^{2-}$ species needed two positively charged points on surface of the adsorbent, but as looking carefully there are two Cr elements in $Cr_2O_7^{2-}$ species; thus, it can be stated that one Cr element adsorbs on one positively charged point of the adsorbent's surface. On the other hand, when pH is higher than 5.6, CrO_4^{2-} appears. Although both species possess two negative charges, CrO_4^{2-} contains only one Cr element while the other consists of two Cr elements. Another important reason is that pH_{pzc} of the adsorbent is 6.5 (Figure 8). The surface charge of the adsorbent becomes less positive when pH increases from 1.0 to 6.5. After this point, the surface charge is more negative, and becomes dominant in alkaline pH solution. From all above viewpoints, the change of pH solution from acidic to basic range causes the decrease in Cr(VI) ions adsorption on surface of the adsorbent.

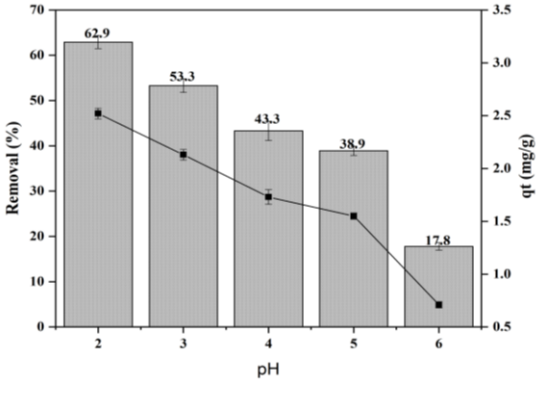

Figure 9. Effect of pH on Cr(VI) adsorption (C_o=20 mg/L, m_{NaY}=0.1 g, T=30°C, V= 20 mL, t=1 h, shaking speed=150 rpm)

3.4.2. Effect of contact time and kinetics

When using nano-adsorbents or porous adsorbents to adsorb pollutant species, it is necessary to keep the adsorbents in contact with bulk solution for a deserved time to let these species condense on surface of the adsorbents. In this study, effect of contact time is conducted in a time range from 0.5 to 6 h and its result is presented in Figure 10. There is a significant increase in adsorption performance from 0.5 to 2 h from 38.5% to 74.5%. However, the performance keeps nearly unchanged from 2 h to 6 h because 2 h of contact time is enough to reach equilibrium of adsorption (Liu et al., 2019). A quick adsorption at the first 2 h in this study is caused by initially fully vacancy on surface of adsorbent and a tiny size of adsorbent. However, the improvement in adsorption efficiency from 2 h to 6 h is insignificant because the adsorption centre covered most of the area, thus it takes longer for Cr(VI) ions to permeate into the capillary pores.

To examine the adsorption rate of Cr(VI) on NaY zeolite, the PFO equation and PSO equation are applied. The adsorption kinetic data of Cr(VI) on NaY zeolite are listed in Table 2. The linear regression coefficients (R^2) of the two hypothetical equations (PFO model: y= -1.12x +0.63, PSO model: y=0.31x+0.11) are both high, showing that the experimental and mathematical model predictions coincide well. Similar to previous study, the PSO offers a better description of adsorption kinetics since the R^2 value of the PSO is greater than that of the first-order (Liu et al., 2019). The equilibrium adsorption capacity (q_e) of PSO equation is 3.24 mg/g, fitting to the experimental equilibrium adsorption capacity of 3.02 mg/g. The adsorption rate of Cr(VI) ions by NaY zeolite occurs with the rate constant of 3.48 g/mg.h.

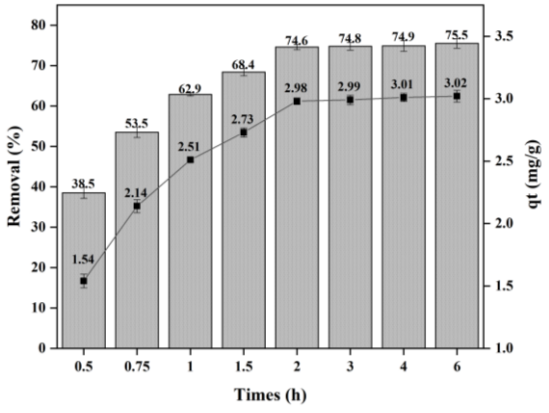

Figure 10. Effect of contact time on Cr(VI) adsorption (C_o=20 mg/L, m_{NaY}=0.1 g, T=30°C, V= 20 mL, pH =2.0, shaking speed=150 rpm)

Table 2. Kinetic model parameters of Cr(VI) adsorption on NaY zeolite

Kinetic models	q_e (mg/g)	k_1 (L/h)	k_2 (g/mg.h)	R^2
Pseudo-first-order	1.89	1.12	-	0.977
Pseudo-second-order	3.24	-	3.48	0.997

3.4.3. Effect of initial concentration and adsorption isotherm

Figure 11 shows the effect of initial concentration on adsorption of Cr(VI) on NaY zeolite. As the concentration of Cr(VI) varies from 10 to 30 mg/L, the adsorption capacity rises sharply from 1.49 to 4.26 mg/g. In the meantime, the adsorption efficiency remains almost unchanged at approximately 74% during the variation of Cr(VI) concentration. This may be explained because at low concentrations, Cr(VI) ions in the solution after certain time of adsorption is very little; it, therefore, takes longer for these ions to condense onto the adsorbent surface (Yusof et al., 2010). At high concentrations, Cr(VI) ions are easily maintained on surface of the adsorbent because of a sufficient number of adsorption sites for the ions. However, it is not feasible to entirely remove Cr(VI) ions in a specific amount of material, thus the adsorbents virtually take their position while Cr(VI) ions remain plentiful in the solution. Maximum sorption capacity of the adsorbent was 9.18 mg/g compared to other studies, the maximum adsorption capacity is 3.56 mg/g (Yusof et al., 2010), the maximum adsorption capacity is 5.6 mg/g (Ghosh et al., 2013).

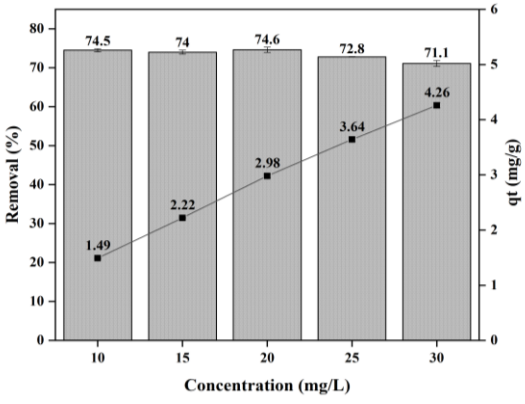

Figure 11. Effect of initial concentration on Cr(VI) adsorption (pH=2.0, m_{NaY}=0.1 g, T=30°C, V= 20 mL, t=2 h, shaking speed=150)

In order to obtain the saturate capacity q_m of Cr(VI) adsorption on NaY zeolite, the Langmuir and Freundlich are widely used and the adsorption isotherm data are presented in Table 3. The linear regression coefficients (R^2) for the Langmuir (y = 0.053x + 1.528) and Freundlich (y = 0.868x – 0.167) isotherm models in Table 3 are 0.815 and 0.989, respectively. With K = 0.409 (L/mg) in the range of 0-1, the adsorption process is favorable and reversible, according to the Langmuir model. When n = 18.76 or 1/n = 0.053, the adsorption process is fairly good since the slope of the straight line is quite low for the Freundlich model. The Freundlich model has a higher linear regression coefficient compared to Langmuir model, indicating that the adsorption process of Cr(VI)) on NaY zeolite follows the Freundlich adsorption isotherm. In other words, the adsorption energy on the surface is not uniform and the adsorption process is reversible.

The Temkin isotherm and Dubinin-Radushkevich isotherm are applied to express adsorption interaction and adsorption mechanisms (Dada et al., 2012). In this study, Temkin isotherm (y= 2.252x - 0.822) and Dubinin-Radushkevich isotherm (y=-4.193x +1.473) had adsorption energy constants of 1.502 and 0.345 kJ/mol, respectively. Both of them are less than 8 kJ/mol, showing that Cr(VI) has a weak interaction with Zeolite NaY, or that physical adsorption is the primary adsorption process in this research (Dada et al., 2012).

Table 3. Adsorption isotherm model parameters

Parameters	Lang.[1]	Freund.[2]	Temkin	R-R[3]
q_{max} (mg/g)	9.18	--	--	--
K (L/mg)	0.41	33.73	--	--
n	--	18.76	--	--
R^2	0.815	0.989	0.757	0.951
K_T (L/g)	--	--	12.49	--
E (kJ/mol)	--	--	1.50	--
β	--	--	--	4.29
q_m	--	--	--	4.36

Note: 1:Langmuir; 2:Freundlich; 3 Dubinin-Radushkevich

4. CONCLUSION

This investigation successfully recovers silica dioxide from unburnt RHA with NaOH solution of 4 M at 90°C for extraction time of 4 h, and synthesizes NaY zeolite using one-pot procedure with a 24-h aging and a 24-h crystallization time. From 10 g rice husk ash containing 96% silica, about 3 g zeolite NaY can be synthesized. This work presents a reducing time, chemical and energy consumption approach for synthesizing NaY zeolite from RHA. Based on the as-synthesized NaY

zeolite, an evaluation of its adsorption capacity is conducted with Cr(VI) ion in aqueous solution. The optimum conditions for Cr(VI) adsorption on NaY zeolite is at pH 2.0 with initial concentration of 20 mgCr/L for 2 h. The adsorption kinetic shows a good agreement with the pseudo-second-order equation, while adsorption isotherm of Cr(VI) on NaY zeolite fits to Freundlich model. A physical adsorption with weak interaction between adsorbate and adsorbent is obtained based on Temkin and Dubinin-Radushkevich isotherm. These findings show it is feasible to synthesize an efficient adsorbent from RHA with a green and novel approach.

REFERENCES

Alemu, A., Gabbiye, N., & Lemma, B. (2020) Application of integrated local plant species and vesicular basalt rock for the treatment of chromium in tannery wastewater in a horizontal subsurface flow wetland system. *Journal of Environmental Chemical Engineering*, *8*(4), 103940. https://doi.org/10.1016/j.jece.2020.103940

Alemu, A., Lemma, B., Gabbiye, N., Alula, M. T., & Desta, M. T. (2018) Removal of chromium(VI) from aqueous solution using vesicular basalt: A potential low cost wastewater treatment system. *Heliyon, 4*(7), e00682. https://doi.org/10.1016/j.heliyon.2018.e00682

Ali, O. I., Hassan, A. M., Shaaban, S. M., & Soliman, K. S. (2011). Synthesis and characterization of ZSM-5 zeolite from rice husk ash and their adsorption of Pb^{2+} onto unmodified and surfactant-modified zeolite. *Separation and Purification Technology*, *83*, 38–44. https://doi.org/10.1016/j.seppur.2011.08.034.

Álvarez, A. M., Guerrón, D. B., & Calderon, C. M. (2021). Natural zeolite as a chromium VI removal agent in tannery effluents. *Heliyon*, *7*, e07974. https://doi.org/10.1016/j.heliyon.2021.e07974

Dada, A. O., Olalekan, A. P., Olatunya, A. M., & Dada, O. (2012). Langmuir, Freundlich, Temkin and Dubinin–Radushkevich isotherms studies of equilibrium sorption of Zn^{2+} unto phosphoric acid modified rice husk. *IOSR Journal of Applied Chemistry, 3*(1), 38-45. https://doi.org/10.1016/j.envpol.2021.118376

Derbe, T., Temesgen, S., & Bitew, M. (2021). A Short Review on Synthesis, Characterization, and Applications of Zeolites. *Advances in Materials Science and Engineering*, *2021*, 1-17. https://doi.org/10.1155/2021/6637898

Dzyazko, Y. U. S., Mahmoud, A., Lapicque, F., & Belyakov, V. N. (2007). Cr(VI) transport through ceramic ion-exchange membranes for treatment of industrial wastewaters. *Journal of Applied Electrochemistry*, *3*, 209–217. https://doi.org/10.1007/s10800-006-9243-7.

Flores, C. G., Schneider, H., Dornelles, J. S., Gomes, L. B., Marcilio, N. R., & Melo, P. J. (2021). Synthesis of potassium zeolite from rice husk ash as a silicon source. *Cleaner Engineering and Technology*, *4*, 100201. https://doi.org/10.1016/j.clet.2021.100201

Ghosh, A., Ahmed, S., & Mollah, M. (2013). Synthesis and characterization of zeolite NaY using local rice husk as a source of silica and removal of Cr (VI) from wastewater by zeolite. *Bangladesh Journal of Scientific and Industrial Research*, *48*(2), 81-88. https://doi.org/10.3329/bjsir.v48i2.15737

Hadipramana, J., Riza, F.V., Rahman, I. A., Loon, L. Y., Adnan, S. H., & Zaidi, A. M. A. (2016). Pozzolanic characterization of waste rice husk ash (RHA) from Muar, Malaysia. *IOP Conference Series: Materials Science and Engineering*, *160*, 012066. DOI 10.1088/1757-899X/160/1/012066

Hamad, M. A., & Khattab, I. A. (1981). Effect of the combustion process on the structure of rice hull silica. *Thermochimca Acta, 48*(3), 343-349. https://doi.org/10.1016/0040-6031(81)80255- 9.

Haq, I. U., Akhtar, K., & Malik, A. (2014). Effect of Experimental Variables on the Extraction of Silica from the Rice Husk Ash. *Journal of the Chemical Society of Pakistan*, *36*(3), 382-387. https://www.researchgate.net/publication/286071234_Effect_of_Experimental_Variables_on_the_Extraction_of_Silica_from_the_Rice_Husk_Ash#fullTextFileContent

Imran, M., Khan, Z. U. H., Iqbal, M. M., Iqbal, J., Shah, N. S., Ali, S. M. S., Murtaza, B., Naeem, M. A., & Rizwan, M. (2020) Effect of biochar modified with magnetite nanoparticles and HNO_3 for efficient removal of Cr(VI) from contaminated water: A batch and column scale study. *Environmental Pollution*, *261*, 114231. https://doi.org/10.1016/j.envpol.2020.114231

Khan, M. N., & Sarwar, A. (2007). Determination of points of zero charge of natural and treated adsorbents. *Surface Review and Letters*, *14*(3), 461–469. https://doi.org/10.1142/S0218625X07009517

Kordatos, K., Gavela, S., Ntziouni, A., Pistiolas, K. N., Kyritsi, A., & Kasselouri-Rigopoulou, V. (2008). Synthesis of highly siliceous ZSM-5 zeolite using silica from rice husk ash. *Microporous Mesoporous Mater*, *115*, 189–196. https://doi.org/ 10.1016/j.micromeso.2007.12.032.

Liu, H., Zhang, F., & Peng, Z. (2019). Adsorption mechanism of Cr(VI) onto GO/PAMAMs composites. *Scientific Reports*, *9*, 3663. https://doi.org/10.1038/s41598-019-40344-9

Mahmoud, M. E., El-Sharkawy, R. M., & Ibrahim, G. A. A. (2021) Promoted adsorptive removal of chromium(VI) ions from water by a green-synthesized hybrid magnetic nanocomposite (NFe_3O_4Starch-Glu-NFe_3O_4ED). *RSC Advances*, *24*, 14829. https://doi.org/10.1039/D1RA00961C

Mirmohamadsadeghi, S., & Karimi, K. (2020). In Current Developments in Biotechnology and Bioengineering, Resource Recovery from Wastes. *Chapter 21-Recovery of silica from rice straw and husk* (pp. 411-433). Elsevier. https://doi.org/10.1016/B978-0-444-64321-6.00021-5

Mohamed, R. M., Mkhalid, I. A., & Barakat, M. A. (2015). Rice husk ash as a renewable source for the production of zeolite NaY and its characterization. *Arabian Journal of Chemistry, 8*(1), 48-53. https://doi.org/10.1016/j.arabjc.2012.12.013

Murtaza, B., Bilal, S., Imran, M., Shah, N. S., Shahid, M., Iqbal, J., Khan, Z. U. H., Ahmad, N., Al-Kahtani, A. A., ALOthman, Z. A., & Farooq, U. (2023) The study of removal chromium(VI) ions from aqueous solution by bimetallic ZnO/FeO nanocomposite with Siltstone: Isotherm, kinetics and reusability. *Inorganic Chemistry Communications, 154*, 110891. https://doi.org/10.1016/j.inoche.2023.110891

Quintelas, C., Rocha, Z., Silva, B., Fonseca, B., Figueiredo, H., & Tavares, T. (2009). Biosorptive performance of an *Escherichia coli* biofilm supported on zeolite NaY for the removal of Cr (VI), Cd (II), Fe (III) and Ni (II). *Chemical Engineering Journal*, *152*(1), 1110-115. https://doi.org/10.1016/j.cej.2009.03.039

Saceda, J. J. F., Leon, R. L. D., Rintramee, K., Prayoonpokarach, S., & Wittayakun, J. (2011). Properties of silica from rice husk and rice husk ash and their utilization for zeolite Y synthesis. *Química Nova, 34*(8), 1394-1397. https://doi.org/10.1590/S0100-40422011000800018

Sharma, P., Singh, S. P., Parakh, S. K., & Tong, Y. W. (2022). Health hazards of hexavalent chromium (Cr(VI)) and its microbial reduction. *Bioengineered*, *13*(3), 4923-4938. https://doi.org/10.1080/21655979.2022.2037273

Shrestha, R., Ban, S., Devkota, S., Sharma, S., Joshi, R., Tiwari, A.P., Kim, H. Y., Joshi, M. K. (2021). Technological trends in heavy metals removal from industrial wastewater: A review, *Journal of Environmental Chemical Engineering*, *9*, 105688. https://doi.org/10.1016/j.jece.2021.105688

Singh, B. (2018). Waste and supplementary cementitious materials in concrete. Woodhead Publishing Series in Civil and Structural Engineering (Eds.), *13 - Rice husk ash* (pp.417-460). https://doi.org/10.1016/B978-0-08-102156-9.00013-4

Tan, W. C., Yap, S. Y., Matsumoto, A., Othman, R., & Yeoh, F. Y. (2011). Synthesis and characterization of zeolites NaA and NaY from rice husk ash. *Adsorption, 17*, 863–868. https://doi.org/10.1007/s10450-011-9350-6

Thanh, L. H. V., Lan, T. N. P., Quyen, T. T. B., Nam, H. Q., & Hanh, C. L. N. (2020). Adsorption of chromium (VI) ion using adsorbent derived from lignin extracted coir pith. *Can Tho University Journal of Science*, *12*(3), 54-65.DOI: 10.22144/ctu.jen.2020.024

Wang, Y., Du, T., Fang, X., Jia, H., Qiu, Z., & Song, Y. (2019). Synthesis of CO_2-adsorbing ZSM-5 zeolite from rice husk ash via the colloidal pretreatment method. *Materials Chemistry and Physics*, *232*, 284–293. https://doi.org/10.1016/j.matchemphys.2019.04.090.

Wittayakun, J., Khemthong, P., & Prayoonpokarach, S. (2008). Synthesis and characterization of zeolite NaY from rice husk silica. *Korean Journal of Chemical Engineering*, *25*, 861-864. https://doi.org/10.1007/s11814-008-0142-y

Yusof, A. M., Keat, L. K., Ibrahim, Z., Majid, Z. A., & Nizam, N. A. (2010). Kinetic and equilibrium

studies of the removal of ammonium ions from aqueous solution by rice husk ash-synthesized zeolite Y and powdered and granulated forms of mordenite, *Journal of Hazardous materials*, *174*(1-3), 380-385. https://doi.org/10.1016/j.jhazmat.2008.05.134